



Norwegian University of
Science and Technology

Numerical and experimental investigation of the unsteady flow field over a simplified hydrofoil plate

Jasmina Pislevikj

Hydropower Development

Submission date: September 2017

Supervisor: Ole Gunnar Dahlhaug, EPT

Co-supervisor: Carl Werdelin Bergan, EPT

Norwegian University of Science and Technology
Department of Energy and Process Engineering

MASTER THESIS

for
Jasmina Pislevikj
Spring 2017

Numerical and experimental investigation of the unsteady flow field over a simplified hydrofoil

Background

The average age of Norwegian hydropower plants is 45 years. Many of these hydropower plants show signs of fatigue and need to be constantly maintained or refurbished. Additionally, some power plants in Norway have experienced failures on new Francis turbine runners. The main problem is the formation of cracks in the turbine runner.

The main challenges for the numerical analysis of the Fluid-Structure Interaction (FSI) on high head Francis turbines originate in the natural frequency of the turbine runner and the fluid properties of the existing pressure oscillations.

Recently, researchers in the Waterpower Laboratory at the Norwegian University of Science and Technology (NTNU) have designed their own high head Francis turbine. Both geometry and model performance data have been published to assist other researchers with relevant case to work on it and also to promote the Francis-99 workshops. The Francis-99 workshops aim to determine the state of the art in high head Francis turbine simulations (flow and structure) under steady and transient operating conditions as well as promote their development and knowledge dissemination openly.

One of the biggest contributions to blade failure is believed to come from Rotor Stator Interaction (RSI). A blade cascade test rig resembling that of a Francis turbine runner has been set up in the Waterpower Laboratory at NTNU in order to investigate the pressure pulsations resulting from the RSI. In order to understand how the dynamic properties of the hydrofoil change with water velocity, pressure measurements are to be taken at several locations in the test rig and analysed. These measurements will be used as the basis for Computational Fluid Dynamics (CFD) validation, as well as for understanding the dynamic properties of the hydrofoil.

Objective

Measurements and numerical analysis of flow from a vibrating hydrofoil installed in a blade cascade test rig for the various flow rates.

The following tasks are to be considered

1. Literature study
 - a. Pressure pulsations in high head Francis turbines
 - b. Dynamic measurements of submerged hydrofoils
 - c. Pressure measurements, signal processing and FFT
2. Software knowledge
 - a. LabVIEW and MATLAB
 - b. CFD-analysis using ANSYS, CFX
3. Laboratory preparations
 - a. Calibration
 - b. Instrumentation and data acquisition setup
4. Pressure measurements (in conjunction with damping measurements performed in the lab)

-- ” --

Within 14 days of receiving the written text on the master thesis, the candidate shall submit a research plan for his project to the department.

When the thesis is evaluated, emphasis is put on processing of the results, and that they are presented in tabular and/or graphic form in a clear manner, and that they are analyzed carefully.

The thesis should be formulated as a research report with summary both in English and Norwegian, conclusion, literature references, table of contents etc. During the preparation of the text, the candidate should make an effort to produce a well-structured and easily readable report. In order to ease the evaluation of the thesis, it is important that the cross-references are correct. In the making of the report, strong emphasis should be placed on both a thorough discussion of the results and an orderly presentation.

The candidate is requested to initiate and keep close contact with his/her academic supervisor(s) throughout the working period. The candidate must follow the rules and regulations of NTNU as well as passive directions given by the Department of Energy and Process Engineering.

Risk assessment of the candidate's work shall be carried out according to the department's procedures. The risk assessment must be documented and included as part of the final report. Events related to the candidate's work adversely affecting the health, safety or security, must be documented and included as part of the final report. If the documentation on risk assessment represents a large number of pages, the full version is to be submitted electronically to the supervisor and an excerpt is included in the report.

Pursuant to “Regulations concerning the supplementary provisions to the technology study program/Master of Science” at NTNU §20, the Department reserves the permission to utilize all the results and data for teaching and research purposes as well as in future publications.

The final report is to be submitted digitally in DAIM. An executive summary of the thesis including title, student's name, supervisor's name, year, department name, and NTNU's logo and name, shall be submitted to the department as a separate pdf file. Based on an agreement with the supervisor, the final report and other material and documents may be given to the supervisor in digital format.

- Work to be done in the Waterpower Laboratory
 Field work

Department for Energy and Process Engineering, *February 13th, 2017.*


Ole Gunnar Dahlhaug
Academic Supervisor

Co-Supervisor:

- Carl Bergan

Abstract

This master thesis resulted from the collaboration between the Norwegian University of Science and Technology (NTNU) and the Macedonian Faculty of Mechanical Engineering, part of the “Ss. Cyril and Methodius University”. The collaboration was established through the project named “Quality Improvement of Master programs in Sustainable Energy and Environment (QIMSEE)”. This project aimed at development and establishment of eight new internationally recognized MSc study programs in the field of “Sustainable Energy and Environment” in eight universities within the West Balkan countries. The project is funded through the Norwegian Programme in Higher Education, Research and Development in the Western Balkans, Programme 3: Energy Sector (HERD Energy) for the period 2014-2016.

In this thesis, the behavior of a simplified hydrofoil in an unsteady water flow field is tested. Due to frequent load variations in high head Francis turbines, the runner vanes happen to break. Rotor stator interaction causes vibrations on the runner vanes. To simulate those vibrations in laboratory conditions, the hydrofoil, mounted in a cascade test rig, is excited with piezo electric patches. The experiment in this thesis shows the behavior of the hydrofoil in different water flow velocities. The results are analyzed and conclusions are brought.

Acknowledgement

I would like to thank all the people that supported me and contributed in some way to the accomplishment of this thesis. Firstly, I would like to express a gratitude to my supervisor at NTNU, Professor Ole Gunnar who gave me the opportunity to go through this research process at the water power laboratory at NTNU, and Carl Bergan for leading me through the process. Secondly, it gives me a great pleasure in acknowledging the inspiration and help of my other supervisor from the Faculty of Mechanical Engineering in Skopje, Professor Zoran Markov, who is a great support throughout all my study process and professional life. Thirdly, I would like to thank KAS for their support.

Special thanks to Elena Tomovska for the unconditional help and all the time and effort dedicated on teaching, advising, motivating and inspiring. Additionally, huge thanks to my colleagues from the QIMSEE project Maja, Natasha, Sonja, Bojan, Neda, Monika, Verce and Igor for the insightful comments and suggestions concerning my study, and the great support throughout all the process. Thanks to Thea Karlsen Loken and the colleagues in the water power laboratory for their assistance. Thanks to Vlatko, Elena and Dushica for being great listeners and inspiration, as well as Adi for her special way of supporting me. Finally, my greatest thanks go to my parents and my sister as well as my colleagues from Systems for Enterprise for their understanding, support and motivation during my master studies, and my life.

Contents

Abstract.....	i
Acknowledgement.....	ii
Contents.....	iii
List of figures.....	v
List of abbreviations.....	vi
Nomenclature.....	vi
1. Introduction.....	1
1.1 Rotor-stator interaction.....	2
1.1.1 Pressure pulsation/Vibration.....	3
1.1.2 Damping.....	3
2. Previous work.....	5
3. Theoretical background.....	6
3.1. Stress and strain.....	6
3.2. Natural frequencies.....	7
4. Closed loop measurements.....	9
4.1. Problem overview.....	9
4.2. Experimental set up.....	9
4.2.1. Test rig schematic.....	10
4.2.2. Instrumentation.....	14
4.2.3. Excitation instrumentation.....	15
4.2.4. Measuring instrumentation.....	16
4.2.5. Measurement matrix.....	17
4.2.6. Post processing method.....	19
4.2.7. Defining experimental mode.....	19

4.2.8. Previous related measurements	21
4.3. Numerical analysis	21
5. Results and discussion	23
5.1. Laser Doppler Vibrometer results	23
5.2. Strain gauge results	25
6. Conclusion	26
7. Further work	27
8. References	28
Appendix	a
A. Plotting	a
1. Matlab code for processing of 3 repetitions	a
2. Matlab code for processing of all repetitions	c
B. Graphs	d
1. 3 repetitions	d
2. For all repetitions	h

List of figures

Figure 1. World energy consumption (left), World energy consumption by region (right) in quadrillion Btu, 1990-2040 [2].....	1
Figure 2. Level of dynamic stresses caused by rotor-stator interaction in hydraulic turbine. $RSI = \text{rotor-stator interaction frequency}$, $nq = N \cdot Q^{0.5} / H^{0.75}$; where N is the runner speed in revolutions per minute, Q is the flow rate in $m^3 s^{-1}$, and H is the head in m.[4]	2
Figure 3. Frequencies observed in a hydraulic turbine[4]	3
Figure 4. System consisted of a block, a spring and a damper subjected to harmonic force $F = F_0 \cos \Omega t$ [5]	3
Figure 5. System consisted of a block, a spring and a damper, where the free end of the spring is forced to move according to $x_s = x_0 \cos \Omega t$ [5]	4
Figure 6. Tensile testing curve for mild steel	7
Figure 7. System overview	10
Figure 8. Simplified schematic diagram of pipe loop for the cascade test rig [20].....	11
Figure 9. Process controlling interface.....	11
Figure 10. Test rig schematic [17]	12
Figure 11. Main parts of the rig [17]	13
Figure 12. Cross section of the test section in AnsysSpaceClaim	13
Figure 13. Hydrofoil dimensions [20].....	14
Figure 14. The simplified hydrofoil with the measuring and exciting parts.....	14
Figure 15. Test section with instrumentation location	15
Figure 16. Piezoelectric patch and driver module	16
Figure 17. Measuring instrumentation set up.....	16
Figure 18. Laser Doppler Vibrometer head	17
Figure 19. Frequency sweep of the hydrofoil from 500 Hz to 2000 Hz [17]	20
Figure 20. FRFs from a test with two different excitation amplitudes	21
Figure 21. Representative graphs of 3 repetitions measured with the LDV (first, middle, last) at four different flow speeds.....	24
Figure 22. Representative graphs of 3 repetitions measuring strain gauge response (first, middle, last) at four different flow speeds.....	25

List of abbreviations

OECD–The organization for Economic Co-operation and development

RSI – Rotor-stator interaction

CFD – Computational Fluid Dynamics

BEP – Best Efficiency Point

Nomenclature

F – Force	N
F_0 – Constant force	N
Ω – Constant forcing frequency	rad/s
m – Mass	kg
x – Displacement	m
k – Kinetic energy	J
ξ – The normalized damping coefficient	-
ω – The natural frequency of the system	rad/s
x_0 – The static elongation of the spring	m
σ – Stress	Pa
ϵ - Strain	-

1. Introduction

The utilization of various renewable sources and different new technologies for electricity production resulted in instabilities in the electricity grid. In order to cover the instability, a need for off-design operation of the hydro power plants has rose. Consequently, the inappropriate handling of the existing turbines resulted in failures. Decreasing the damages and providing resistant turbine design is one of the inspiration for creating the Francis-99 project[1]. As a minor part of the Francis-99 project, the idea for examining the simplified hydrofoil behavior in an unsteady flow field was created.

Francis turbines are one of the most prevalent types used in the hydropower plants in Norway, where more than 95% of the electricity production comes from hydro energy. Renewables performance are not an object of research anymore, as the energy demands are growing fast, the urge for their development and stronger reliability is obvious, as well as confirmed in the world energy consumption projections presented in the International energy outlook 2016[2] created from U.S. Energy Information Administration. The consumption is expected to increase for 71% from 2012 to 2040 in the Non-OECD countries, while in OECD countries for 18%, and on global level it is 48% (Figure 1).

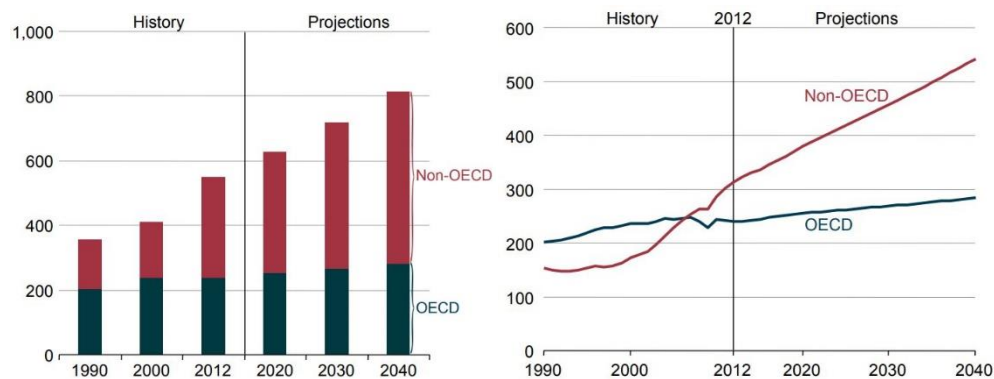


Figure 1. World energy consumption (left), World energy consumption by region (right) in quadrillion Btu, 1990-2040 (2)

Consequently, the high efficiency and the reliability of the technologies is tending to constantly increase the level. In the case of Francis turbine production it means thinner blades which then cause increased vibration amplitudes and damages. The vibration influences and the consequences they are causing are imitated in the designed rig mounted at the Water power

laboratory at the Norwegian University of Science and Technology. The behavior of a simplified hydrofoil, subjected to vibration, representing a runner blade, is the case investigated in this work.

1.1 Rotor-stator interaction

Catastrophic blade damages can occur due to the high amplitude pressure pulsation from the rotor-stator interaction (RSI). The failures are mostly resulting from the induced high cycle fatigue on the blades[3]. The ratio of the stress amplitudes from rotor-stator interaction to the total dynamic stress is shown on Figure 2, as one half the peak-to-peak amplitude for different runner types. The presented values are based on the strain gauge measurements on Francis turbines, at rated operating conditions[4].

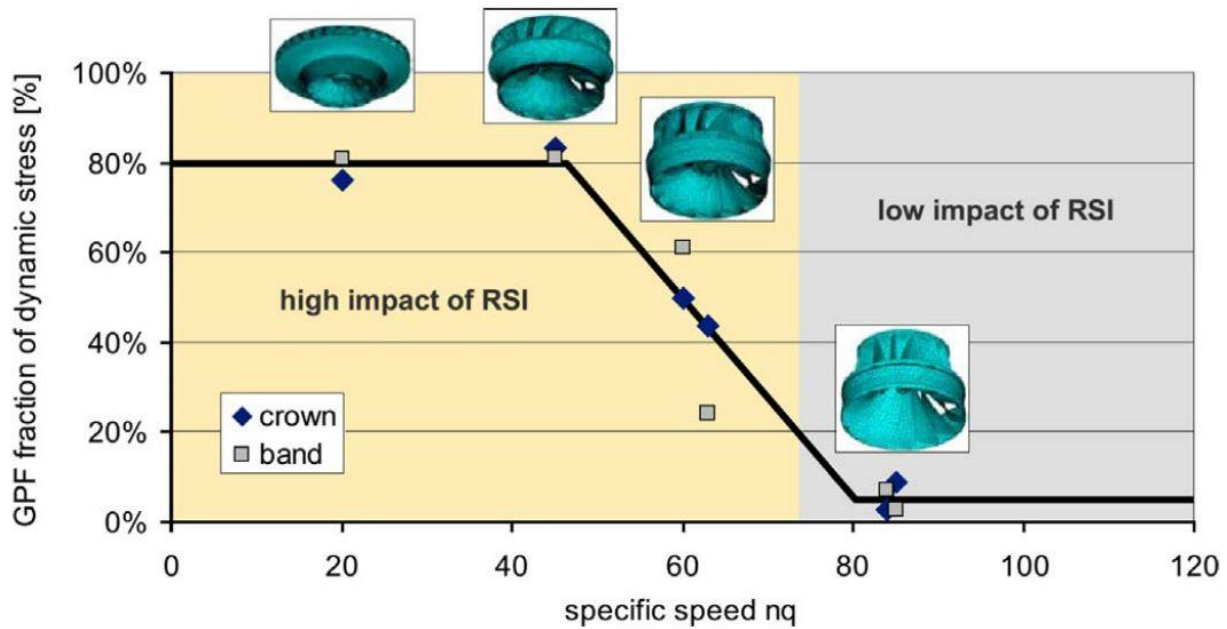


Figure 2. Level of dynamic stresses caused by rotor-stator interaction in hydraulic turbine. $RSI = \text{rotor-stator interaction frequency}$, $nq = N \cdot Q^{0.5} / H^{0.75}$; where N is the runner speed in revolutions per minute, Q is the flow rate in $m^3 s^{-1}$, and H is the head in m.[4]

1.1.1 Pressure pulsation/Vibration

Brief overview of the flow induced vibration are shown on the diagram on Figure 3. The flow-induced vibrations are mainly associated with the draft tube vortex rope, Von Karman vortices¹, turbulence, cavitation and rotor-stator interaction[4].

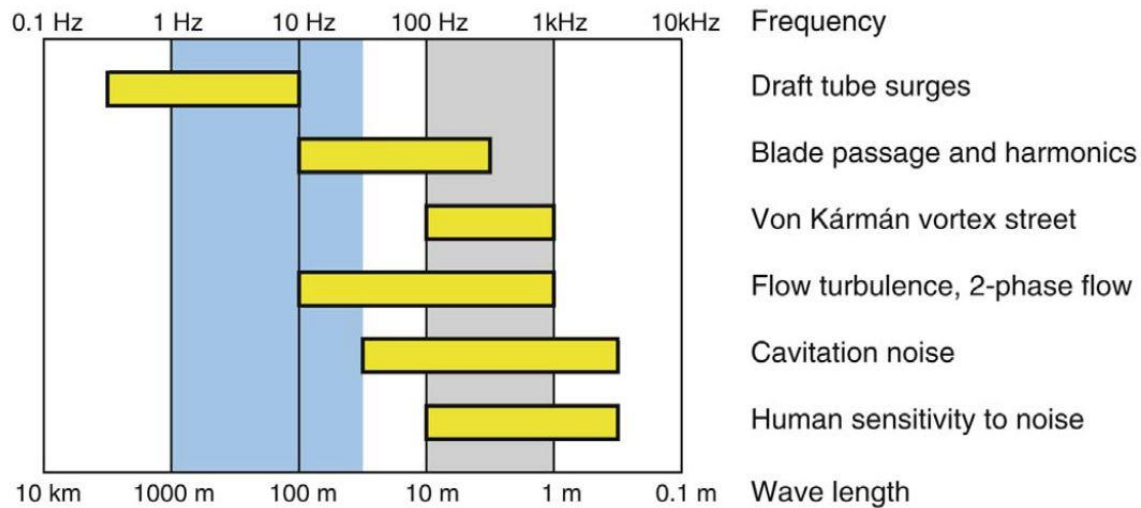
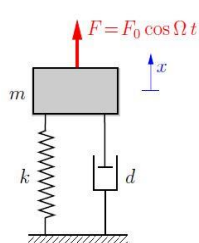


Figure 3. Frequencies observed in a hydraulic turbine[4]

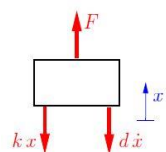
1.1.2 Damping

Briefly about damping can be most easily explained from the theory of dynamics, review from the “Engineering mechanics 3, Dynamics”.



A whole case for excitation through a force or via a spring is explained, as stated in “Dynamics”[5]. System consisted of a block, a spring and a damper as shown on Figure 4 is taken into consideration. The block is subjected to a harmonic force $F = F_0 \cos \Omega t$, where Ω is a given constant forcing frequency.

The equation of motion is obtained as:



$$m\ddot{x} = -kx - d\dot{x} + F_0 \cos \Omega t \rightarrow m\ddot{x} + d\dot{x} + kx = F_0 \cos \Omega t \quad 1-1$$

Figure 4. System consisted of a block, a spring and a damper subjected to harmonic force $F = F_0 \cos \Omega t$ [5]

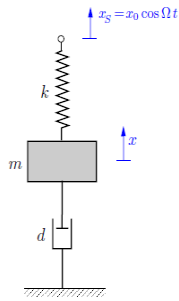
¹Frank M. White, Fluid Mechanics 4th edition, McGraw-Hill Series in Mechanical Engineering, page 295

If the abbreviations, as follows are introduced,

$$2\xi = \frac{d}{m}, \omega^2 = \frac{k}{m}, x_0 = \frac{F_0}{k} \quad 1-2$$

the differential equation is obtained:

$$\ddot{x} + 2\xi \dot{x} + \omega^2 x = \omega^2 x_0 \cos \Omega t \quad 1-3$$



Where:

- constant ξ – the *normalized damping coefficient*,
- ω – the *natural frequency of the system* and
- x_0 – the *static elongation of the spring* which is caused by a constant force

F₀.

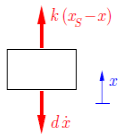


Figure 5. System consisted of a block, a spring and a damper, where the free end of the spring is forced to move according to $x_s = x_0 \cos \Omega t$ [5]

The system in Figure 5 will be considered. In this case, the free end of the spring is forced to move according to: $x_s = x_0 \cos \Omega t$.

It is important to note that no external force acts on the block. Then the elongation of the spring is given by: $x_s - x$ which leads to the equation of motion for the block:

$$m\ddot{x} = k(x_s - x) - d\dot{x} \rightarrow m\ddot{x} + d\dot{x} + kx = kx_0 \cos \Omega t \quad 1-4$$

With the abbreviations (Eq. 1-2) is again obtained:

$$\ddot{x} + 2\xi \dot{x} + \omega^2 x = \omega^2 x_0 \cos \Omega t$$

Thus, the motions of the blocks of both systems are described by the same equation.

2. Previous work

The dampening effect is a complex problem that has been widely experimented on simplified hydrofoils, while it is still not fully understood on the whole turbine. What makes it knotty, are the wide range of phenomena that are raising up from the broad range of operating conditions[6]. An immersed vibrating structure includes structural and material - total dampening.

In order to predict the dampening effect, many simplified setups, analogues to a hydraulic turbine have been investigated. The highest interest is on the trailing edges and shapes of the hydrofoil, which are also used as a starting point for the research done in this thesis. The dampening effect that the water have on vibrating hydrofoils with different trailing edges and profiles shape help in defining the experiment properties.

As stated in Tahereh at al. work[7], the hydrodynamic dampening effect is known as the fluid contribution to the total dampening of a system. Various shapes are tested in order to define the response and reasons for its occurrence. Their main aim is to decrease the structural vibration and vortex shedding amplitudes. Some examples of diversity of trailing edges used are using oblique trailing edge[8], or the so called Donaldson trailing edge[9]. It has been noticed that both significantly reduce the flow induced vibrations. The motion of pitching hydrofoils has been investigated by[10] in order to catch the vibration that may be caused from the flow fields, where also the formation of a laminar separation bubble, creating on the hydrofoil surface, has been considered. Flow induced vibrations has been produced, together with reduced lift, lowered deformations, increased drag and decreased lift from a cavitating flow over a hydrofoil in the experiment obtained in [11].

3. Theoretical background

The main issue investigated in the work is the frequency response of the hydrofoil in water flow field. In order to present it, it is necessary to measure it according to the behavior, which is based on vibrating of the structure. It means, the stress and the strain of the material can be followed on one side, while on the other side, with the equipment available, the velocity of the vibration of the hydrofoil is captured.

Shortly, a brief theory related to the issue elaborated in this thesis is given below

3.1. Stress and strain

The equations 3-1 and 3-1 define the mechanical stress and strain[12], respectively.

$$\sigma = \frac{F}{A_0} \quad 3-1$$

$$\epsilon = \frac{\Delta l}{l_0} \quad 3-2$$

Stress and strain exert the behavior of proportionality, (Eq. 3-3), as long as the yield strength of the material is not reached.

$$\sigma = E\epsilon \quad 3-3$$

Strain can be defined as: *a measure of deformation representing displacement relative to a reference length*. Stress and strain may cause permanent deformations and ultimately fracture on materials. Figure 6 shows, the typical strain diagram, tensile testing curve, for mild steel.

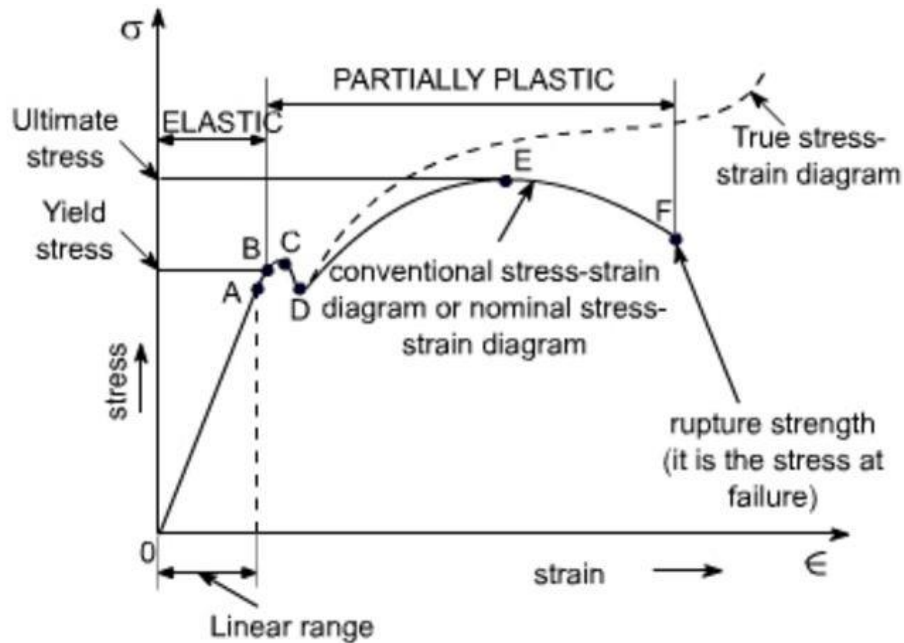


Figure 6. Tensile testing curve for mild steel²

Material properties such as the yield and ultimate strength determines the amount of stress and strain the material can handle without permanent deformations and cracks forming. For a ductile material the fracture strength is lower than the ultimate strength.

The slope of the curve is the Young's Modulus of the material as long as the yield strength is not reached. Once the yield strength of the material is reached, the behavior of mechanical stress to strain changes and as the ultimate strength is reached, fracture is possible.

3.2. Natural frequencies

When designing the mechanical components for a hydropower plant is important to take in consideration the natural frequencies (i.e. eigenmodes) of the system. The off-design turbine running initiate vibration of the equipment. When those vibration frequencies coincide with the natural frequency of the system, an increase of stress and strain is produced as a result of amplification of the vibrations[13].

²<http://www.nptel.ac.in/courses/Webcourse-contents/IITROORKEE/strength%20of%20materials/lects%20&%20pics/image/lect11/lecture11.htm> (accessed 15.07.2017)

Explanation of natural frequency can go as so: imagining simple degree of freedom system of a mass hanging on a spring, where x is the direction of movement. Equation 3-4 present the motion of the system.

$$m\ddot{x} + kx = 0 \quad 3-4$$

Moreover, multiple degree of freedom system is described adding mass and stiffness matrix (Eq. 3-5)

$$M\ddot{x} + Kx = 0 \quad 3-5$$

These lead to mass-normalized-stiffness matrix (Eq. 3-6)

$$\tilde{K} = M^{-\frac{1}{2}}(KM)^{-\frac{1}{2}} \quad 3-6$$

The eigenvalues and eigenvectors can be obtained by solving the equation of the algebraic eigenvalue problem which based on the above mentioned equations can be defined as shown in Eq. 3-7:

$$\tilde{K}v = \lambda v \quad 3-7$$

The above presented procedure describes the basic concept of obtaining the natural frequencies of a system. Complex geometries and dampening add complexity to the calculation and the use of numerical tools may be helpful when obtaining the natural frequencies[14].

4. Closed loop measurements

4.1. Problem overview

Flexible electricity demand leads to frequent starts and stops of the hydro power plants which push them to extreme operating limits. This also means unfavorable load at which the turbines are run, causing material fatigue and turbine failures. Also, frequent rotor-stator interactions are initiated from the variable operation which cause unpleasant vibration for the vanes. It can often result with cracks, which are one of the culprits for the turbine failure. Different turbine designs have different response on the operating conditions. More precisely, the design of every vane play one of the main roles of the turbine efficiency and its resistance on variable flow regimes.

The flow conditions inside the hydraulic turbine runner are most important for providing secure and reliable operation of the plant. When running above the best efficiency point (BEP), periodic flow phenomena occurs, which can be amplified and cause damage to mechanical equipment[14]. Due to rotor – stator interaction, a high amplitude pressure pulsation is induced, it hits the runner blades and there is crack formation, as the fatigue cycles exceeds the threshold limit. In High Head Francis turbines failures arise because the pressure pulsations are close to the natural frequency of the runner[15], [16].

4.2. Experimental set up

The flow velocity effects on damping and the natural frequency of a hydrofoil have been studied in specially designed test rig[17]. This section focuses on the physical setup of the rig, the instrumentation used with corresponding calibration and the test matrix used during the experimental campaign.

In this case, defining the test matrix was done experimentally based on the previous measurements. At some velocities, cavitation was occurring. Preventing cavitation inside the test rig was done with operating under high pressure. P. Ausoni et al.[18] presented more about the effect of cavitation on fluid structure interaction, and also stated that due to the vibration amplitude, additional vorticity is occurring and that leads to an early cavitation inception. The maximum pressure limit on the piping system inside the laboratory is 10 bar, while the height difference between the test rig system and the pump is 11 m. In order to achieve the desired water velocity in the test section, the speed of the main pump used for the testing is regulated.

4.2.1. Test rig schematic

A test rig has been designed and installed at the Waterpower Laboratory at NTNU Trondheim which is one of the oldest laboratories, dating back from 1917[19]. Image overview is shown on Figure 7, where the test rig position is labeled with red circle. On Figure 8, a schematic diagram of the pipe loop is shown[20]. The main section of the system used is the pump system that has the following specification:

Maximum head	100 m
Open system head	16 m
Maximum flow	1,0 m ³ /s
Maximum power	600 kW
Operation in both open and closed loop	

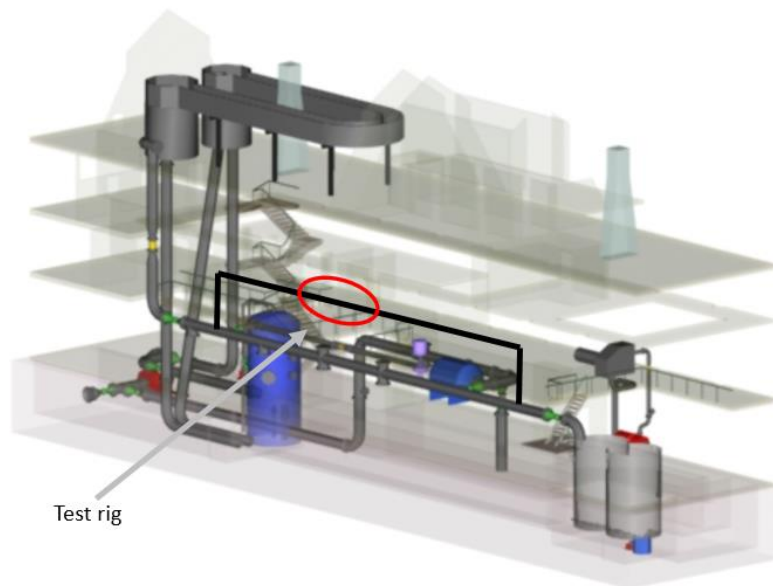


Figure 7. System overview³

³ Power point presentation from the Waterpower laboratory at NTNU Trondheim, okt05

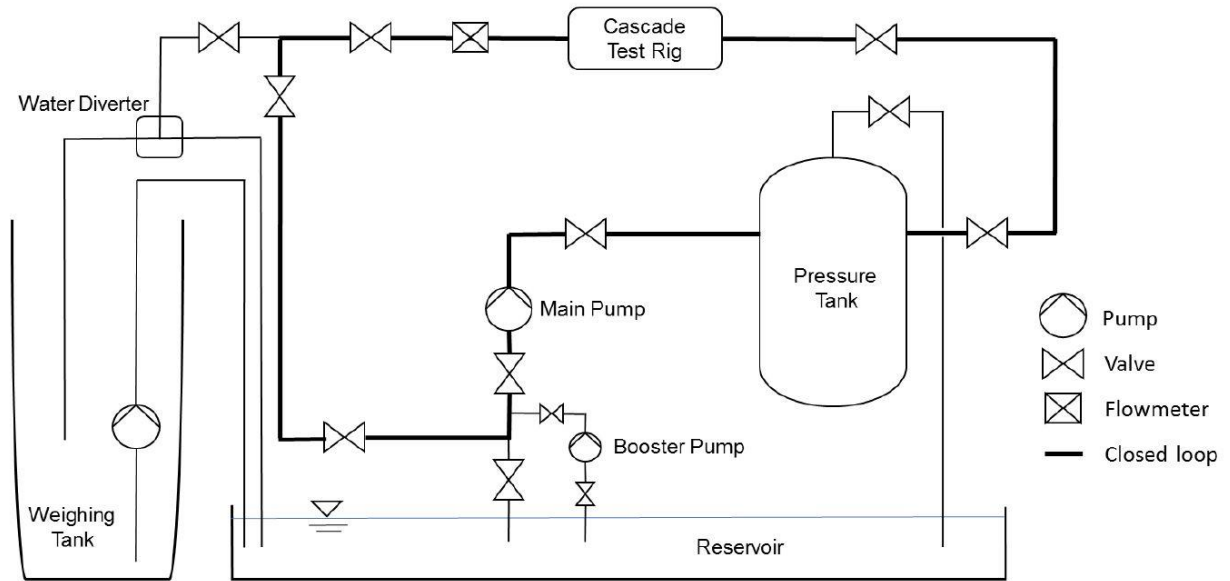


Figure 8. Simplified schematic diagram of pipe loop for the cascade test rig[20]

On Figure 9, the distance controlling system is shown.

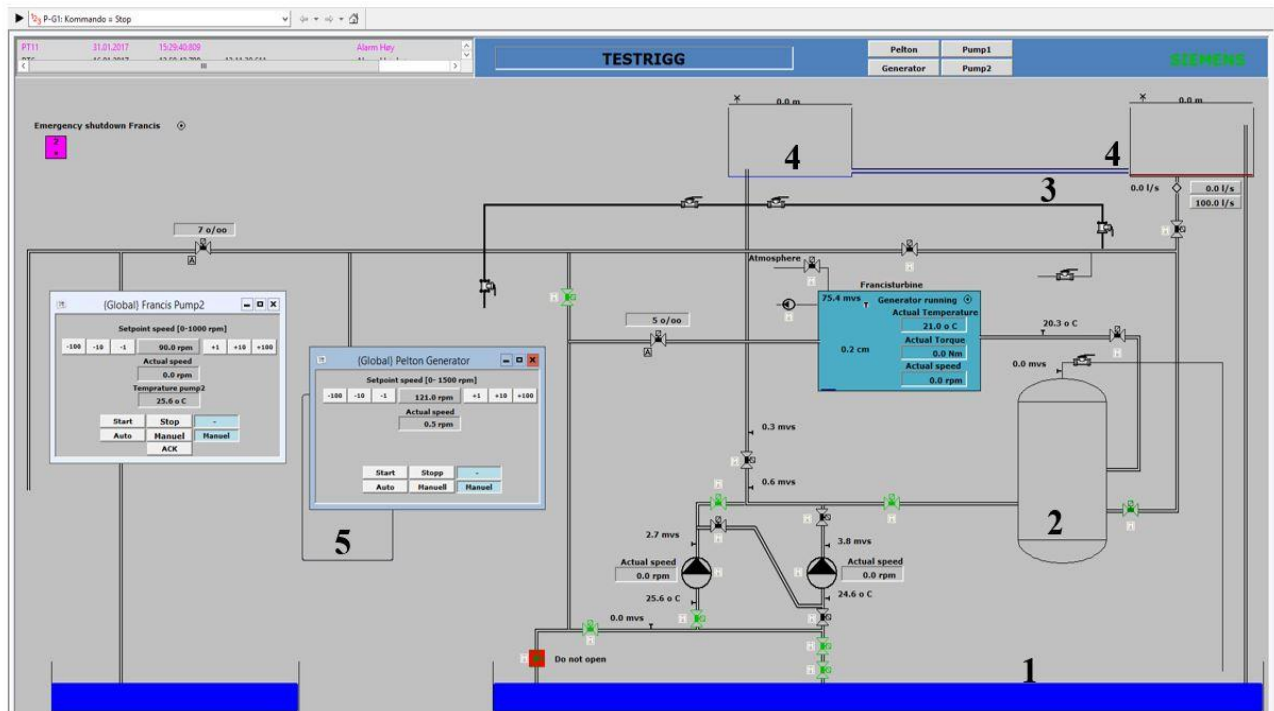




Figure 9. Process controlling interface

Legend:

1	Sump
2	Pressure tank
3	Test rig position
4	Attic reservoirs for open loop testing
5	Weighing tank
	Valves
	Pumps

The additional booster pump that is part of the system is controlled manually.

The design of the test rig is thoroughly described in the paper “Design and experiment”[21], and only the main features are shown in the content below. The test rig has been installed in the internal piping system at the Waterpower Laboratory and the flow is delivered by one of the main pumps.

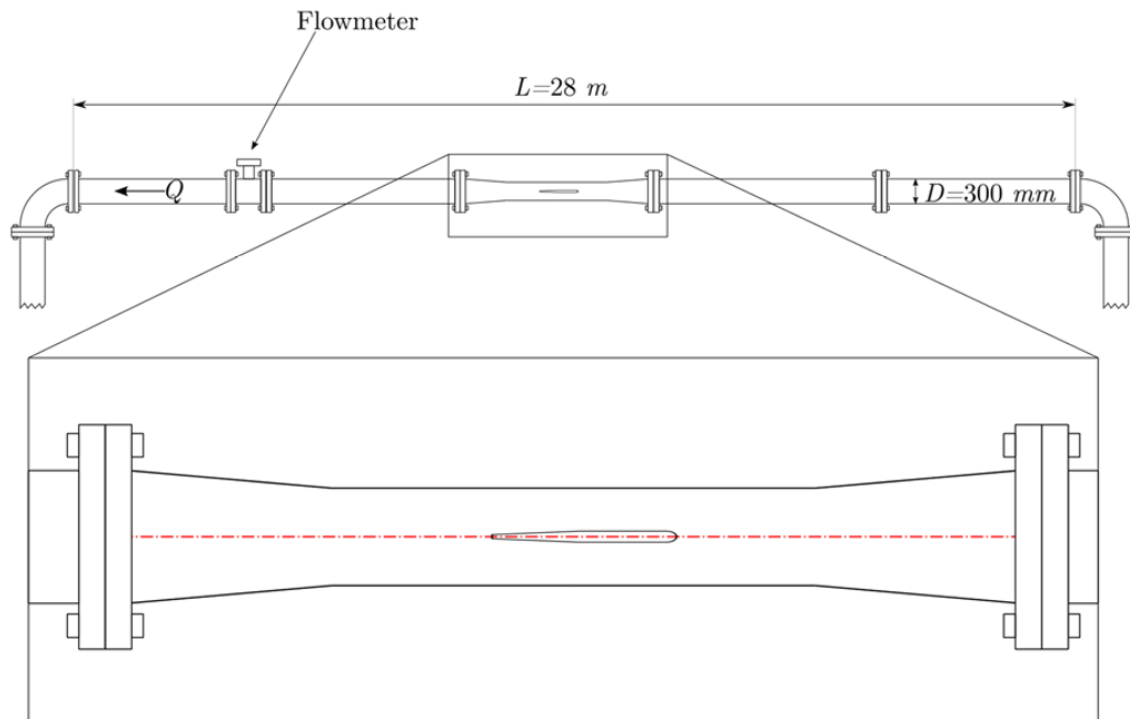


Figure 10. Test rig schematic[17]

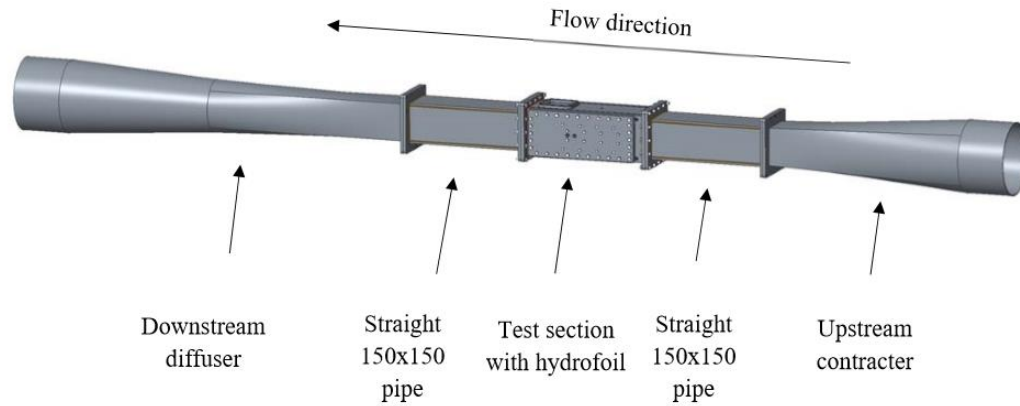


Figure 11. Main parts of the rig[17]

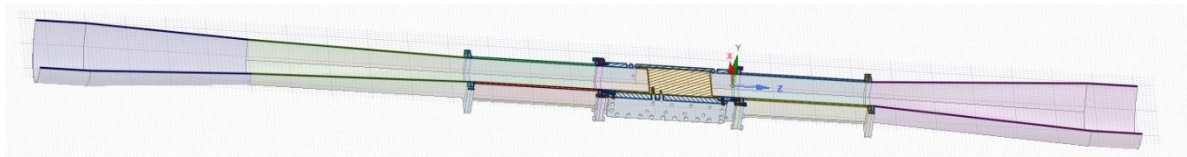


Figure 12. Cross section of the test section in AnsysSpaceClaim

The test rig is comprised of an upstream section where the velocity increases and downstream diffuser which change the pipe section from 300 mm diameter pipe to a square 150 mm x 150 mm, measured internally. The test section where the hydrofoil is located, along with most of the instrumentation, is placed between two straight pipe sections in order to isolate the test section from the effects of the cross section change. The hydrofoil cassette, i.e. the hydrofoil and the side walls, is bolted to the test section with 16 bolts on the front and back, which are all tightened with 5 Nm of torque. To enable visual study inside the section, it is equipped with Plexiglas windows, both from the top and from the bottom of the section where the hydrofoil is placed. The bottom window is also used for the measurements with the Laser Doppler Vibrometer.

The hydrofoil is custom made. Its design aims to narrow down the quantity of parameters that could possibly influence the characteristics of the flow across the hydrofoil. The dimensions of the hydrofoil are shown on Figure 13.

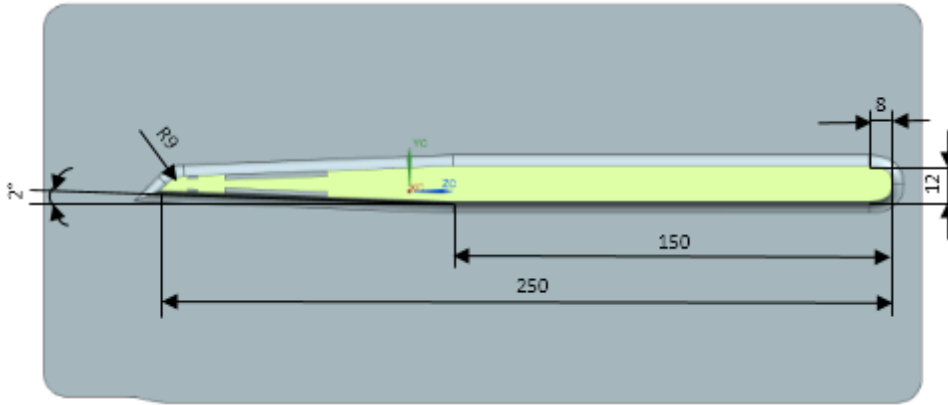


Figure 13. Hydrofoil dimensions[20]

The design is made in order to have zero angle of attack with chord length of 250 mm. Maximum thickness of 12 mm is applied. In order to avoid additional forces on the hydrofoil, the suction and the pressure surfaces of the hydrofoil are symmetrical and they are flat chambers starting from the leading edge. Making it similar as in Francis turbine, the hydrofoil is fixed on the both sides. The oblique of the trailing edge, is the so called Donaldson trailing edge. On its advantage in terms of hydrodynamic damping and vortex-induced vibrations it is explained in [22] and in [8].

4.2.2. Instrumentation

Instrumentation within the test section include both measuring and exciting parts. The hydrofoil is excited by two piezoelectric patches placed at the center of the foil close to the trailing edge, shown on Figure 14.

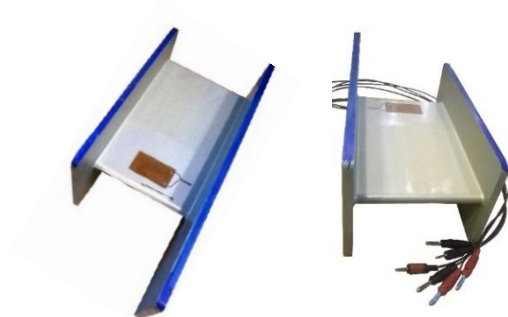


Figure 14. The simplified hydrofoil with the measuring and exciting parts

To measure the response of the hydrofoil a set of semiconductors based strain gauges are mounted on each side of the hydrofoil's trailing edge. In addition, a Laser Doppler Vibrometer (LDV) is mounted below the test section, with optical access to the trailing edge. Cables for the patches and strain gauges exit the test section through tunnels in the hydrofoil while the laser measures through the lower Plexiglas window. Response to the vibrations by the water are measured by multiple dynamic pressure transducers installed mainly to provide validation data to the numerical simulations. Detailed overview on the Figure 15.

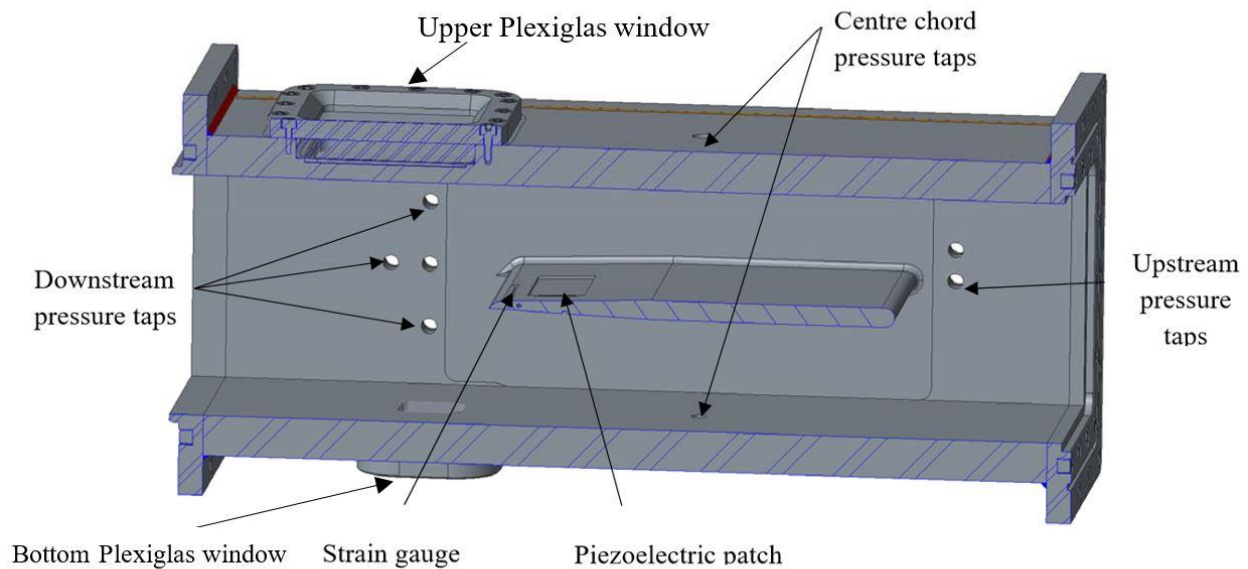


Figure 15. Test section with instrumentation location

The material of the hydrofoil is aluminum alloy with the following properties:

Density: $\rho = 2810 \text{ kg/m}^3$

Young's modulus: $\varepsilon = 7.17 \cdot 10^{10} \text{ Pa}$

Poisson ratio: $\nu = 0.33$

4.2.3. Excitation instrumentation

The piezoelectric patches are controlled by LabVIEW through amplifiers, and can be excited by any signal pattern. Piezoelectric patches are of the type P-876.A15 DuraAct Patch Transducer as seen in Figure 16 along with the driving module.

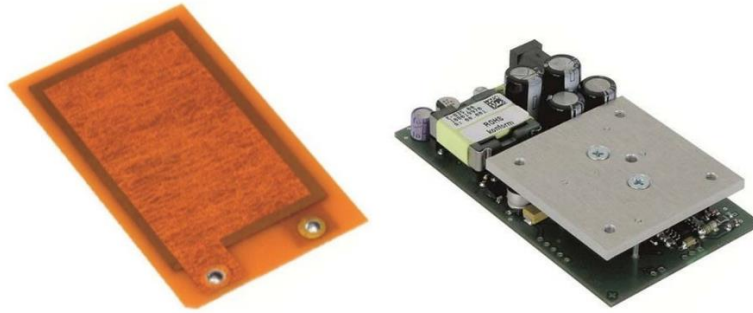


Figure 16. Piezoelectric patch and driver module

As the piezoelectric patches are driven by a high voltage signal supplied by a E-835 DuraAct Piezo Driver Module. The module used has an output voltage range of -100 to 250 V at a peak power of 30 W. The driver module is controlled by a -4 to 10 V signal generated by an NI9236 Analog Output module from National Instrument.

4.2.4. Measuring instrumentation

The response of the hydrofoil caused by the excitation force is measured in two different forms; *surface velocity and strain*.

The physical set-up from the lab is shown on Figure 17.



Figure 17. Measuring instrumentation set up

Strain in the hydrofoil close to the trailing edge is measured by a doublet of semiconductor strain gauges mounted on each side of the hydrofoil, and connected to a Wheatstone bridge. The strain gauges are of the type Kulite S/UCP-120-090. These semiconductor strain gauges have previously been compared with a conventional strain gauge, and was found to be substantially more sensitive[23].

The velocity of the hydrofoil close to the trailing edge is measured by a Laser Doppler Vibrometer (LDV) from Polytec of the type OFV 2200, with an optical head of type OFV-303. The LDV's optical head is shown in Figure 18.



Figure 18. Laser Doppler Vibrometer head

4.2.5. Measurement matrix

The measurements were performed at different water flow velocities, starting at 0 m/s up to 27,5 m/s. For each velocity, 30 measurement repetitions were performed before moving on to the next tested flow velocity (on 26 m/s only 3 repetitions were performed because only the temperature increase was following, which rose for 2° C after three repetitions). In order to capture the dynamic properties of the hydrofoil with an acceptable uncertainty, repetitions at each velocity were prioritized over a high resolution in the velocity range.

The following list summarizes the measurements performed:

- 0 m/s: 30 repetitions
- 4 m/s: 30 repetitions
- 8 m/s: 30 repetitions

- 10 m/s: 30 repetitions
- 13 m/s: 30 repetitions
- 15 m/s: 30 repetitions
- 16 m/s: 30 repetitions
- 17 m/s: 30 repetitions
- 19,5 m/s: 30 repetitions
- 24 m/s: 30 repetitions
- 26 m/s: 3 repetitions
- 27,5 m/s: 30 repetitions

In addition, measurements were performed without blade excitation at each velocity in order to assess the levels of vibration without excitation.

At every beginning and after finishing the measurements at a particular flow velocity, 3 repetitions of measurements for instrumentation control at 0 m/s, were performed.

Before performing measurements with the mentioned input velocities, measurements with flow velocities starting at 0m/s, with steps of 5m/s up to 25m/s had been performed. A measurement with lower excitation amplitudes had been performed at 5m/s, in order to assess if the damping ratio is in any way dependent on the excitation amplitude. For each velocity, 30 measurement repetitions had been performed before moving to the next flow velocity (at 25m/s, only 24 repetitions had been performed, due to the onset of cavitation). To capture the dynamic properties of the hydrofoil with an acceptable uncertainty, repetitions at each velocity had been prioritized over a high resolution in the velocity range.

The measurements performed at:

- 0m/s : 30 repetitions
- 5m/s : 30 repetitions
- 5m/s, amplitude-altered : 30 repetitions
- 8m/s : 30 repetitions
- 10m/s : 30 repetitions
- 5m/s : 30 repetitions
- 20m/s : 30 repetitions

- 25 m/s : 24 repetitions

At the time of these measurements the temperature had not been taken into consideration, even though it has been measured, hence its influence is not noticed in the previous results. Due to the importance of possible temperature effect on the hydrofoil behavior, since the temperature will have influence on the water density, these measurements show the temperature influence measured through the analysis process. The temperature is measured using a thermocouple attached on the pipe, insulated from outside influences, placed before the test section. The tests have been done by the rule that the temperature should not vary more than 5°C during the test.

4.2.6. Post processing method

Each repetition of each measurement is post-processed separately, and treat as separate measurement. The resulting spread in results will be used to evaluate the damping raising up in the hydrofoil behavior. Each frequency step in each repetition is analyzed in the frequency domain using Welch's power spectral density estimate[24]. The flattop window is chosen for its accuracy in estimating the amplitude. For determining the phase delay between the input and output signal, the cross-power spectral density is used with the Hanning window[25]. This process yields the amplitude magnification and the phase delay of the output signal compared to the input signal for one frequency step. This process is performed for all the frequency steps in one measurement. The amplitude and phase information can be expressed as an imaginary number, and this will, when done for all the frequency steps in one measurement, generating a Frequency Response Function (FRF)[13] for the measurement.

From the FRF, the damping factor can be estimated in a number of ways. For these analysis, the circle fit method[26], also known as the method of Kennedy and Pancu, will be used. The circle fit method consists of plotting the real parts of the FRF vs. its imaginary parts. This is called a Nyquist plot, and it will form a circle when passing through a resonant peak. A circular curve fit can then be applied to the data, and this circle can be used to estimate parameters such as damping ratio.

4.2.7. Defining experimental mode

One single frequency sweep from 500 Hz to 2000 Hz yields three distinct peaks, as seen in Figure 19. The numerical results indicate that the peaks found are indeed the first three blade

bending modes. Further measurements have then been focused on the region 500-700 Hz, as this is the region of the first blade-bending mode.

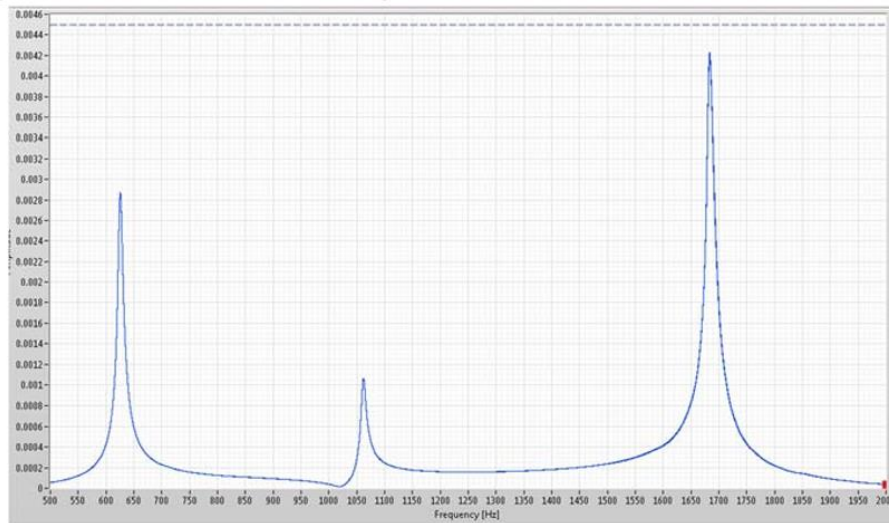


Figure 19. Frequency sweep of the hydrofoil from 500 Hz to 2000 Hz[17]

Each measurement consists of the following steps:

1. Measure the vibration of the hydrofoil without excitation for 30s
2. Perform a 60s linear frequency sweep from 500-700 Hz
3. Use the sweep to find the natural frequency of the foil, and generate a list of frequencies to excite in order
4. Excite each of the frequencies generated in (3), one at a time, for 5s
5. Repeat (4) 30 times

LDV measurements are used to reconstruct the FRFs. The largest measured deflections were measured without moving water, with deflections of approx. 0.04 mm. From the FRFs, the damping factor can be estimated, and plotted as a function of water velocity (Figure 20).

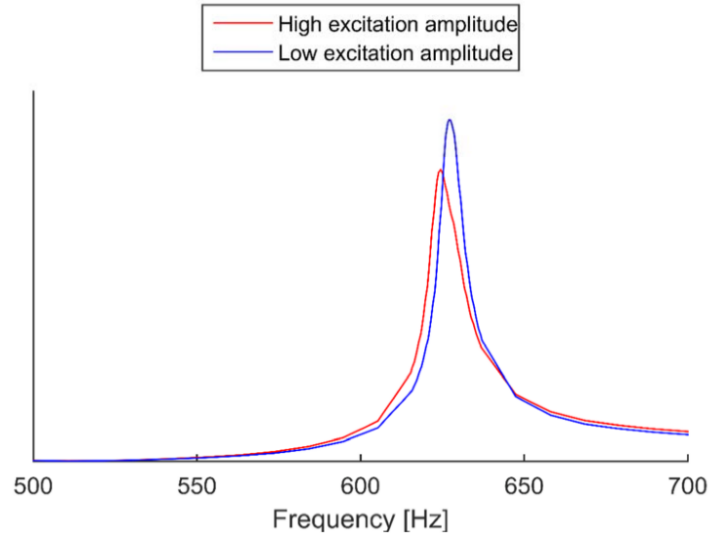


Figure 20. FRFs from a test with two different excitation amplitudes

This alteration in excitation amplitude yielded an altered natural frequency, and an altered damping ratio. For the two measurements, the results were:

- Low excitation: $f_n = 627.1 \text{ Hz} \pm 0.5 \text{ Hz}$, $\zeta = 0.00540 \pm 0.00015$
- High excitation: $f_n = 624.2 \text{ Hz} \pm 0.1 \text{ Hz}$, $\zeta = 0.0069 \pm 0.0001$

4.2.8. Previous related measurements

Limited in time and resources, for this thesis, only the excitation measurements following the temperature variations, has been done. More on the instrumentation used previously, the pressure measurements, calibration and uncertainty analysis is described in the related thesis: “Study of vortex shedding from a vibrating hydrofoil”, as created in [20].

4.3. Numerical analysis

Based on the physical set-up, a numerical investigation using the numerical fluid dynamics tool CFX has been performed in a project work [27] which is further developed in a thesis in order of geometry and experimental improvement. As already noticed with the experimental set-up, there is a standing out frequency at a flow rate of $0,25 \text{ m}^3/\text{s}$ of $635,2 \text{ Hz}$, which seems like vortex shedding coincides with the natural frequency, called lock – in effect. At flow rate of $0.25 \text{ m}^3/\text{s}$, the numerical investigation shows a frequency peak at 321.7 Hz , which is close to the experimental one that stand out on $302,6 \text{ Hz}$ at $0,18 \text{ m}^3/\text{s}$ flow rate. Even though this effect is noticed both in the numerical simulations and the experimental ones, a direct comparison cannot

be performed. Defining specific comparable frequencies is very difficult, because the experimental investigation is noisier than the numerical ones. On the other side, taking in consideration that only one-way fluid structure investigation has been performed, it is insufficient to compare it to the experimental measurements.

5. Results and discussion

Transferring the experimental measurements into visible results have been done with calculation of the Frequency-response functions (FRFs). Representative selection is shown on the graphs below. Additionally, all the rest relevant results are shown in Appendix.

The frequency response of the time domain data gathered from the measurements, has been found, using the following method:

1. Find the excitation amplitude, using FFT with the welch method, using the flattop window⁴
2. Find the response amplitude, using FFT with the welch method, using the flattop window
3. Find the phase delay between the excitation and response, using the cross-power spectrum
4. Calculate the amplitude factor as amplitude out divided by amplitude in
5. Format the amplitude + phase as complex numbers.

Using the above mentioned procedure, one FRF was generated. In order to achieve the total number of results, this procedure was repeated for each measurement.

The observation of the hydrofoil behavior was made by both, following the movement of the material caused by the vibration with Laser Doppler Vibrometer, and by spotting the strain occurring on the material. As the work in [20] shows more about the general behavior of the hydrofoil in similar conditions, in this thesis the influence of the temperature is mainly in the focus of observation.

5.1. Laser Doppler Vibrometer results

From the graphs shown below (Figure 21), it can be noticed that the temperature is not constant throughout the entire process of the measurement performed at particular flow speed. The temperature difference during the measurement, which lasted around 150 minutes, increased for around 2°C, mainly initiated from the heating up of the pumps, as well as from the friction between the pipes and the fluid, and the influence of the ambient temperature. A cross section of three representative repetitions has been chosen, the first the middle one and the last one. The script can be found in Appendix.

⁴ H. Schmid, *How to use the FFT and Matlab's pwelch function for signal and noise simulations and measurements*, Institute of Microelectronics, FHNW/IME, August 2012

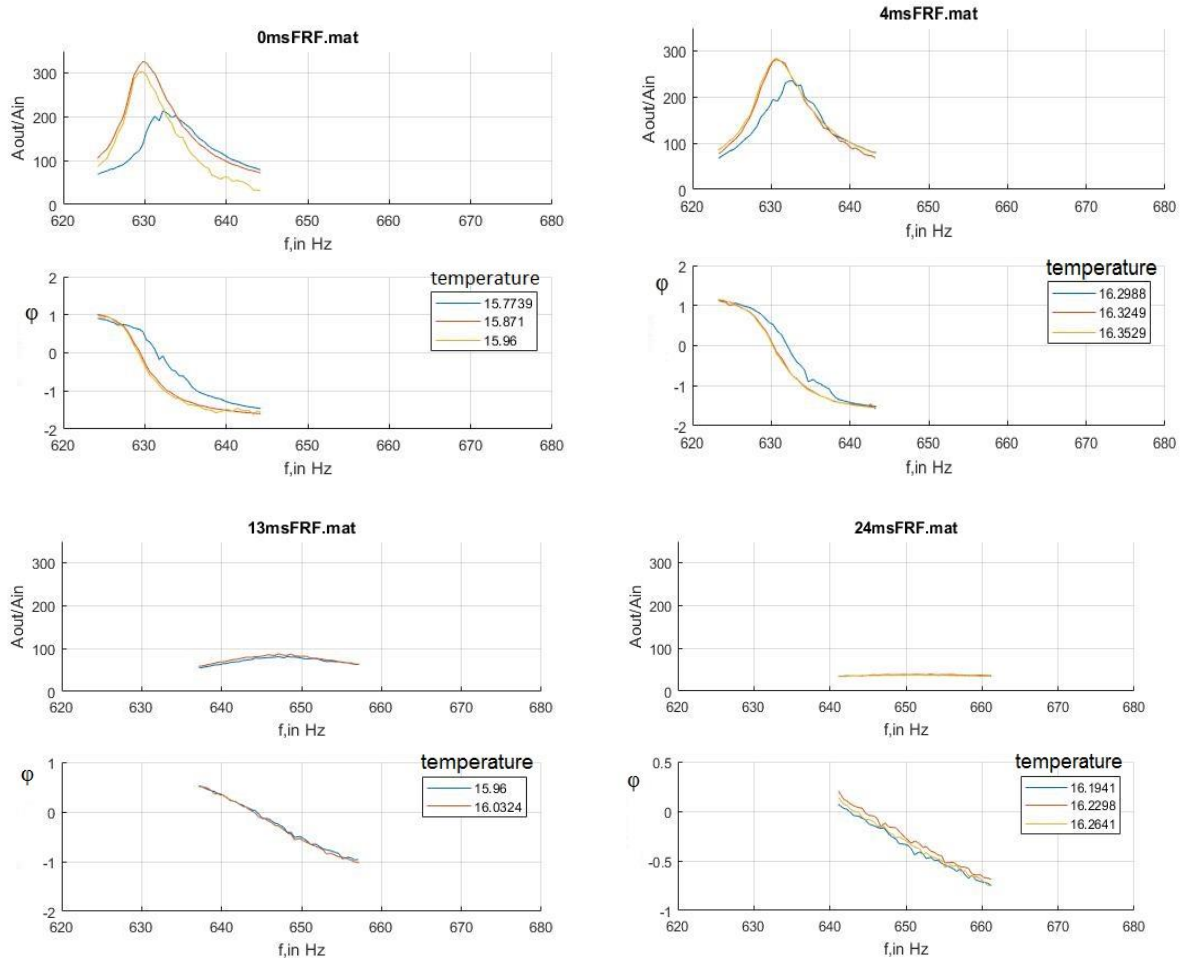


Figure 21. Representative FRF graphs of 3 repetitions measured with the LDV (first, middle, last) at four different flow speeds

The slower the flow speed of the fluid, the higher bending of the hydrofoil is caused from the forced vibration. As the flow speed rises, consequently the pressure decreases and dampening of the hydrofoil is noticed. This behavior is most likely expected to be happening as a result of the hydrofoil shape, especially the geometry of the trailing edge and the lower surface. As the lower surface is straight, unlike the upper that is curved, the pressure distribution is different from low to higher speeds.

When it comes to temperature influence, it cannot be said that significant concession are caused. However, as the graphs show, at lower speeds the first repetition, the one on the lowest temperature, is a bit further away from the other two, and also indicates less bending, but considering all the other experiment conditions, any distinct conclusion cannot be brought.

Even though each measurement has been performed each in different period, aiming to have same/similar starting temperature, differences in the starting temperature occurred as a result of the ambient temperature. Evident temperature rise is noticed at high speeds, like 26 m/s and higher, when the temperature changed at the very beginning in only 3 repetitions. The influence of the heating up of the pumps is here clearly confirmed, as the pump was running with 750 rpm and higher. Consequently, at this flow speed, only 3 repetitions were done, which are not taken as representative samples.

5.2. Strain gauge results

Like at the results from the LDV, these results show the same way of bending and behavior on the working temperature. Hence, the graphs are looking similar.

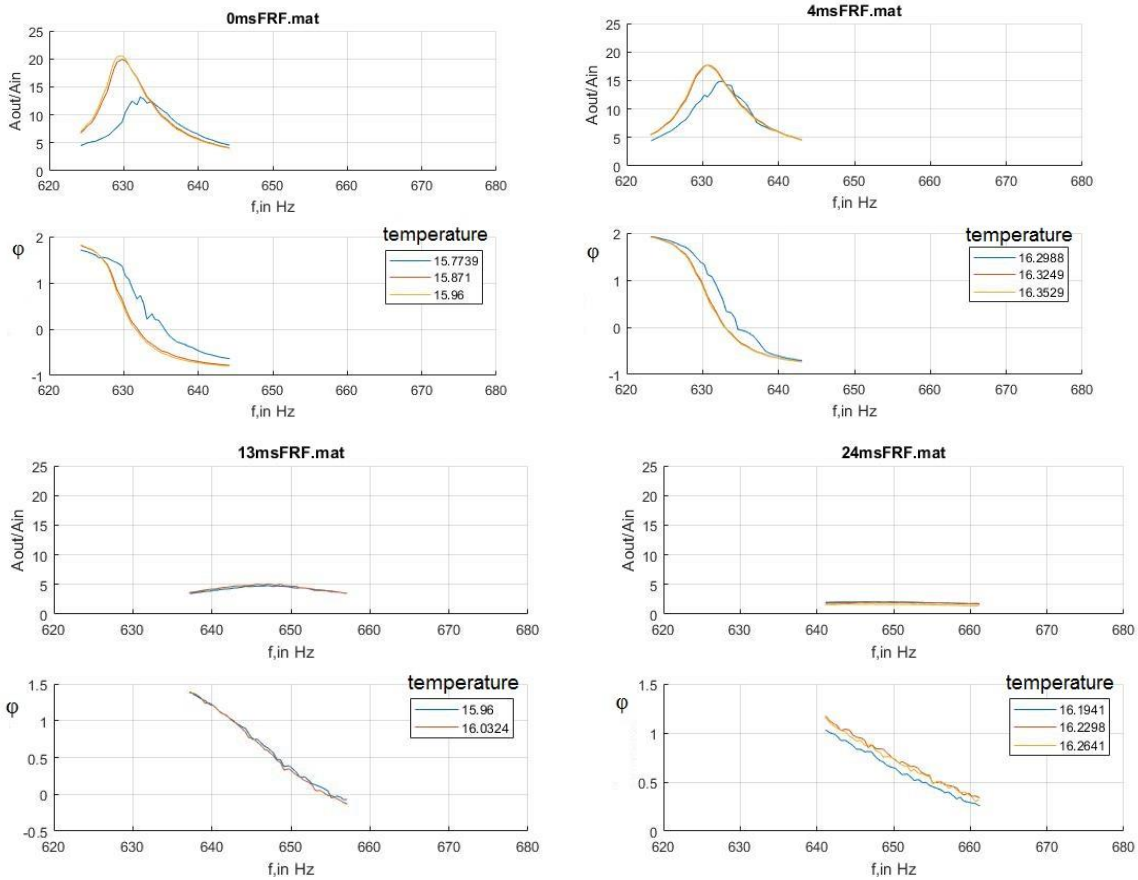


Figure 22. Representative graphs of 3 repetitions measuring strain gauge response (first, middle, last) at four different flow speeds

6. Conclusion

In this Master thesis, the idea of observing the temperature influence on the hydrofoil behavior, did not yield with any significant results. One important remark is that the natural frequency of the hydrofoil did not occur at the same flow velocity during the entire testing procedure. Namely, when performing the experiments, at the moment of increasing the pump speed to reach flow velocities above 11 m/s, the natural frequency of the hydrofoil occurred at 11 m/s. After finishing the testing at the particular flow velocity, the pump speed had to be decreased in order to turn off the system, and at that point the water temperature already had raised for about 2-2.5 [°C]. While decreasing the pump speed, the natural frequency could not be noticed at the same point of flow velocity as in the beginning. Hence, any particular temperature influence cannot be confirmed, as fatigue of material or exhausting of the instrumentation is also a valid explanation of the occurrence.

In short, this hydrofoil geometry (the so called: *Donaldson trailing edge*) and material (aluminum alloy) caused lock in effect (natural frequency of the hydrofoil coming close to the induced one) at the velocity of 11 m/s at flow temperature close to 16 [°C]. This can be taken as a point for further examinations with carefully remarked material's, and measurement instrument properties at the time of performing of the experiment. The flow rate, together with the process of achievement of a desired flow velocity, also proved to be a factor. During the 150 min measurement, for flow rates under 19 m/s, the temperature increased for 2 [°C] and for higher flow rates that increase was 5-8 [°C].

The working temperature used throughout the measurements did not influence the dampening effect. Hence it can be concluded that difference in temperature in range of 3°C is not representative enough for noticing changes in behavior of the hydrofoil.

7. Further work

Being treated in tough conditions, this hydrofoil measurement instrumentation have been destroyed at the end of these testing, hence not direct improvement/further work on this can be done. However, CFD investigation have wide range of testing possibilities and is one of the activities already implemented in[27].

Moreover, one discussed possibility is taking the section away from the closed loop, fill it with water, close both ends and testing the behavior of the hydrofoil in still water, subjected on temperature differences. It means, the hydrofoil will be subjected on vibrations, as in the closed loop, and the water will be either heated up or cooled down. Also, it can either being kept constant, changed, or simply left without any influence but the ambient, and follow the behavior throughout the 30 repetitions.

Additionally, trying to keep constant temperature in the closed loop, which means installation of a cooling system, is another possibility. Anyhow considering the conditions in the laboratory, this may be neither very effective, nor efficient.

Other, unavoidable step, as the shape of the hydrofoil seems to be the main issue of the dampening occurrence, is designing different ones with more symmetric geometry.

8. References

1. *Francis-99 project*. 2017 [cited 2017 28.06]; Available from: <https://www.ntnu.edu/nvks/francis-99>.
2. *International Energy Outlook 2016 With Projections to 2040*. 2016, U.S. Energy Information Administration Office of Energy Analysis U.S. Department of Energy Washington, DC 20585.
3. Huth, H.-J., *Fatigue Design of Hydraulic Turbine Runners*, in *Department of Engineering Design and Materials*. 2005, Norwegian University of Science and Technology (ntnu): Trondheim, Norway. p. 178.
4. Trivedi, C. and M.J. Cervantes, *Fluid-structure interactions in Francis turbines: A perspective review*. *Renewable and Sustainable Energy Reviews*, 2017. **68**(Part 1): p. 87-101.
5. Dietmar Gross, W.H., Jörg Schröder, Wolfgang A. Wall, Sanjay Govindjee, *Engineering Mechanics 3. 2 ed. Dynamics*. 2014, Verlag Berlin Heidelberg: Springer.
6. *HiFrancis*. 2016 [cited 2017 15.07]; Available from: <https://www.ntnu.edu/nvks/hifranicis>.
7. Liaghat, T., *Two-Way Fluid-Structure Coupling In Vibration And Damping Analysis Of An Oscillating Hydrofoil*, in *Département De Génie Mécanique*. 2014, École Polytechnique De Montréal: Montréal.
8. Zobeiri, A., et al., *How oblique trailing edge of a hydrofoil reduces the vortex-induced vibration*. *Journal of Fluids and Structures*, 2012. **32**(Supplement C): p. 78-89.
9. Donaldson, R., *Hydraulic turbine runner vibration*. *ASME J. Eng. Power*, 1956. **78**: p. 1141- 1147.
10. Antoine Ducoin, F.D., Jacques-André Astolfi , Jean-François Sigrist, *Computational and experimental investigation of flow over a transient pitching hydrofoil*. *European Journal of Mechanics*, 2009. **28** (6): p. 728-743.
11. Akcabay, D.T. and Y.L. Young, *Influence of cavitation on the hydroelastic stability of hydrofoils*. *Journal of Fluids and Structures*, 2014. **49**(Supplement C): p. 170-185.
12. Rethwisch, W.D.C.a.D.G., *Fundamentals of materials science and engineering*. Vol. 21. 2013, New York: Wiley
13. Inman, D.J., *Vibration with Control*. 4 ed. 2006, England: John Wiley & Sons Ltd.
14. Leonhardsen, S., *Numerical Investigation of Flow Field subject to Vibrating Structure*, in *Department of Energy and Process Engineering*. 2017, Norwegian University of Science and Technology: Trondheim, Norway
15. Peter Dörfler , M.S., André Coutu *Flow-Induced Pulsation and Vibration in Hydroelectric Machinery*. *Engineer's Guidebook for Planning, Design and Troubleshooting*. 2013, London: Springer.
16. André Coutu, M.D.R., Christine Monette, Bernd Nennemann. *Experience With Rotor-Stator Interactions in High Head Francis Runner*. in *24th Symposium on Hydraulic Machinery and Systems*. 2008. Foz do Iguassu: IAHR.
17. Bergan, C.W., *Design of Experiment for Blade Cascade Measurements, HiFrancis WP 1.1*. 2016, Norwegian University of Science and Technology: Trondheim, Norway.

18. Philippe Ausoni, M.F., François Avellan, Xavier Escaler, Eduard Egusquiza. *Cavitation Effects On Fluid Structure Interaction In The Case Of A 2d Hydrofoil*. in *ASME Fluids Engineering Division Summer Conference*. 2005. Houston, TX.
19. *Waterpower laboratory, Norwegian University of Science and Technology*. 2017 [cited 2017 23.07]; Available from: <https://www.ntnu.edu/ept/laboratories/waterpower>.
20. Ting, M.M.B., *Study of vortex shedding from a vibrating hydrofoil*, in *Department of Energy and Process Engineering*. 2017, Norwegian University of Science and Technology: Trondheim, Norway.
21. Carl Werdelin Bergan, B.W.S., *3D model of the cascade rig*. 2016, Norwegian University of Science and Technology: Trondheim, Norway.
22. Yao, Z., et al., *Effect of trailing edge shape on hydrodynamic damping for a hydrofoil*. *Journal of Fluids and Structures*, 2014. **51**(Supplement C): p. 189-198.
23. Bergan, C.W., *Testing of piezoelectric MFSs in conjunction with semiconductor strain gauges*. 2016, Norwegian University of Science and Technology: Trondheim, Norway.
24. *Welch power spectral density estimate, Matlab*. 2017 [cited 2017 02.08]; Available from: <https://se.mathworks.com/help/signal/ref/pwelch.html>.
25. Fredric, H.J. *Use of windows for harmonic analysis*. in *IEEE*. 1978.
26. T, B., *Fundamentals of Structural Dynamics*. 1993, London: Springer.
27. Leonhardsen, S., *Numerical Investigation of Flow Field subject to Vibrating Structure*. 2016, Norwegian University of Science and Technology: Trondheim, Norway.

Appendix

A. Plotting

Plotting of the data gathered with LabView was done using Matlab.

1. Matlab code for processing of 3 repetitions

```
files = dir('*.mat');
legendText = cell(1,1);

for i = 1 : length(files);
    filename=files(i).name;
    load(filename);

    %nReps = size(F_LDV,1);
    nReps = size(F_strain_M,1);

    figure(i);
    clf;
    hold on;

    for k = 1 : nReps

        % f = F_LDV(k,:);
        % pxy = PXY_LDV(k,:);
        f = F_strain_M(k,:);
        pxy = PXY_strain_M(k,:);

        mag = abs(pxy);
        phas = angle(pxy);

        subplot(211);
        xlabel('f,in Hz');
        ylabel('Aout/Ain');
        hold on;
        if (k == 1 || k == 15 || k == 30)
            plot(f,mag);
            grid on;
        end;

        % xlim([0,400]);
        %ylim([0.5e-3,5.5e-3]);
        ylim([0,25]);
        %ylim ([0,350]);
        xlim([620,680]);
        title(filename);
        subplot(212);
        hold on;
        % plot(f,phas);
```



```
if (k == 1 || k == 15 || k == 30)
    plot(f,phas);
    xlabel('f,in Hz');
    ylabel('Aout/Ain');
    grid on;
end;

xlim([620,680]);

legendText = [legendText; num2str(Twater(k))];

end
legendText(1)=[];
legend(legendText);

end
```

2. Matlab code for processing of all repetitions

```
files = dir('*.*mat');

legendText = cell(1,1);
for i = 1 : length(files)
    filename=files(i).name;
    load(filename);

    nReps = size(F_LDV,1);

    figure(i);
    clf;
    hold on;

    for k = 1 : nReps

        f = F_LDV(k,:);
        pxy = PXY_LDV(k,:);
        % f = F_strain_R(k,:);
        % pxy = PXY_strain_R(k,:);

        mag = abs(pxy);
        phas = angle(pxy);

        subplot(211);
        xlabel('f,in Hz');
        ylabel('Aout/Ain');
        hold on;
        plot(f,mag);
        ylim([0,350]);
        % ylim([0.5e-3,5.5e-3]);
        xlim([620,680]);
        title(filename);
        subplot(212);
        xlabel('f,in Hz');
        ylabel('\phi');
        hold on;
        plot(f,phas);
        xlim([620,680]);

        legendText = [legendText; num2str(Twater(k))];

    end

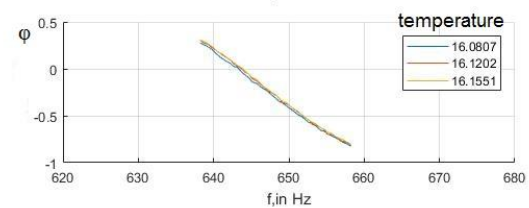
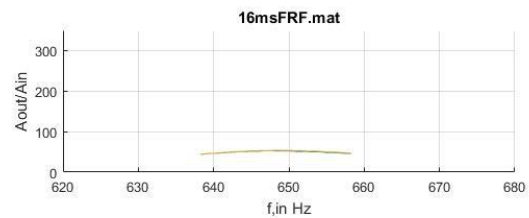
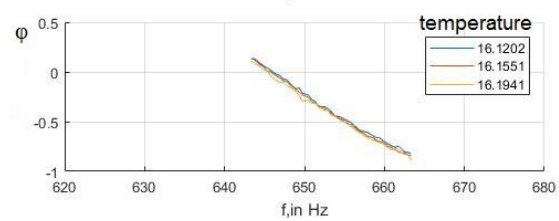
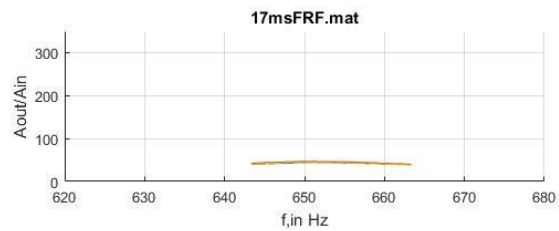
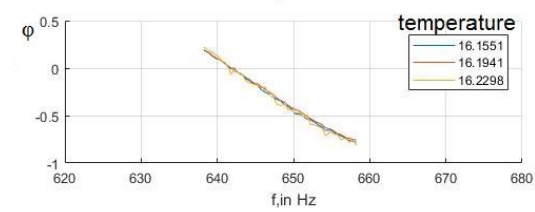
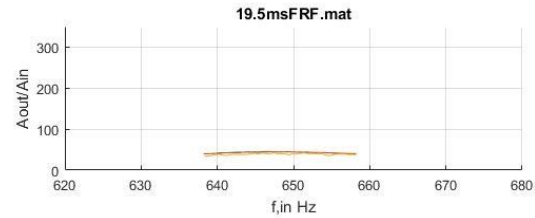
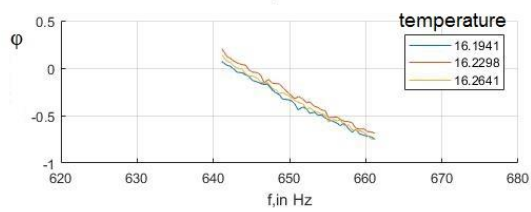
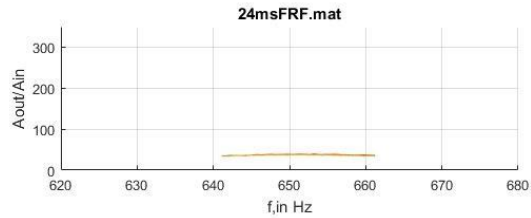
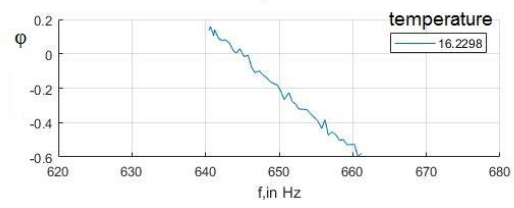
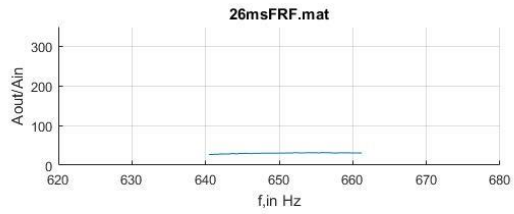
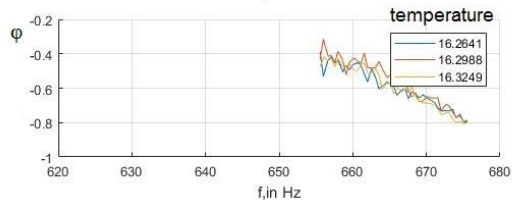
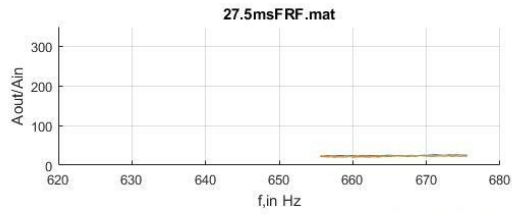
    legendText(1)=[];

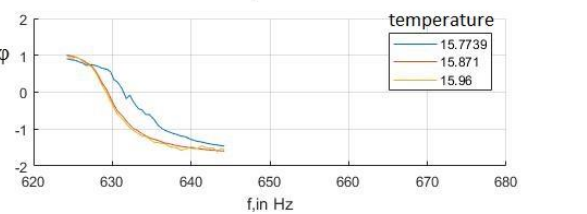
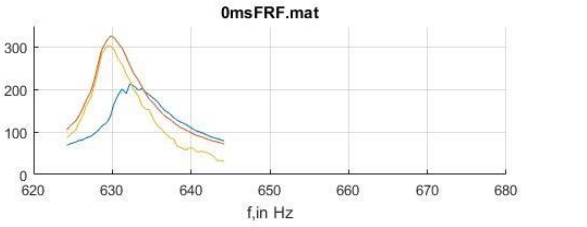
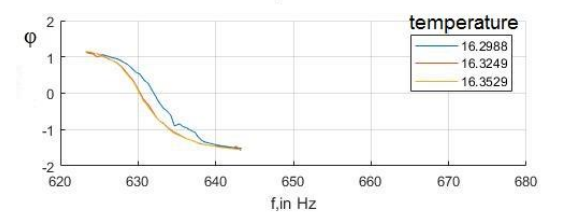
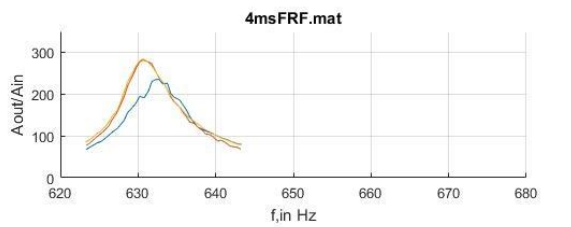
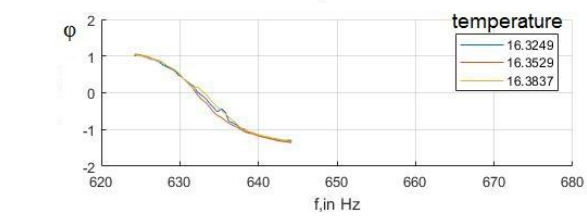
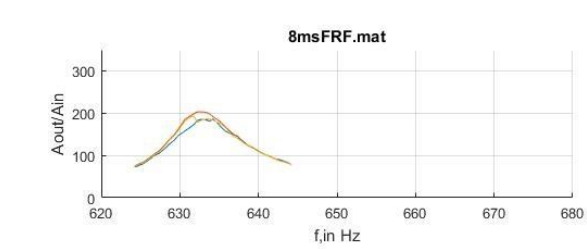
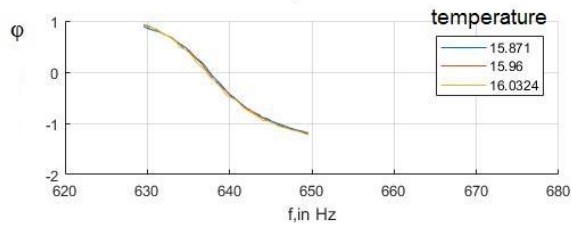
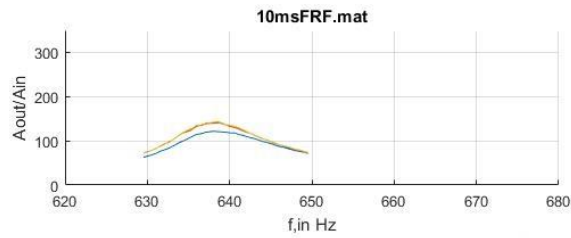
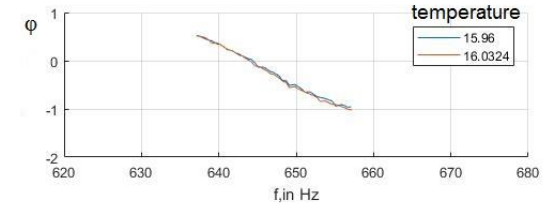
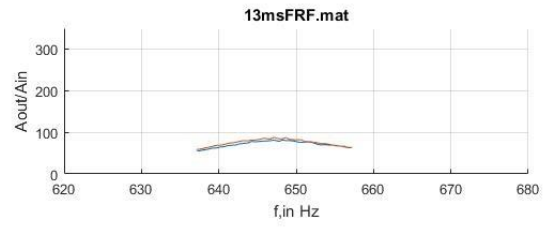
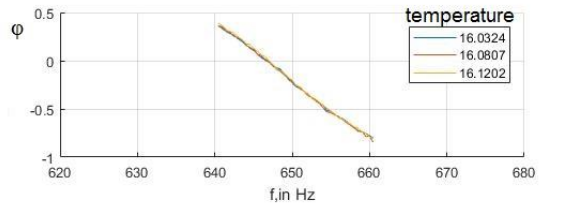
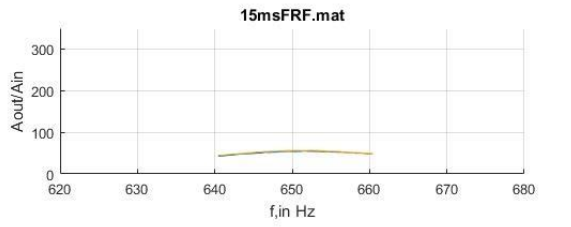
end
```

B. Graphs

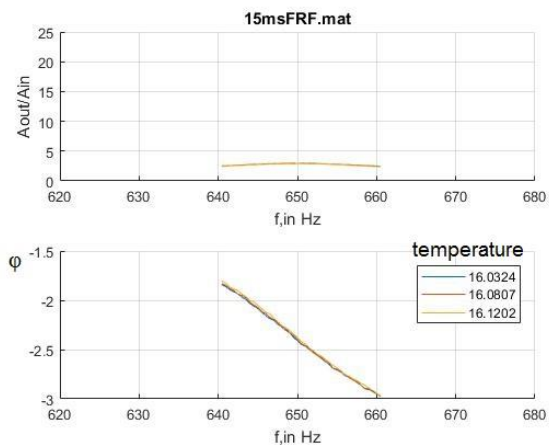
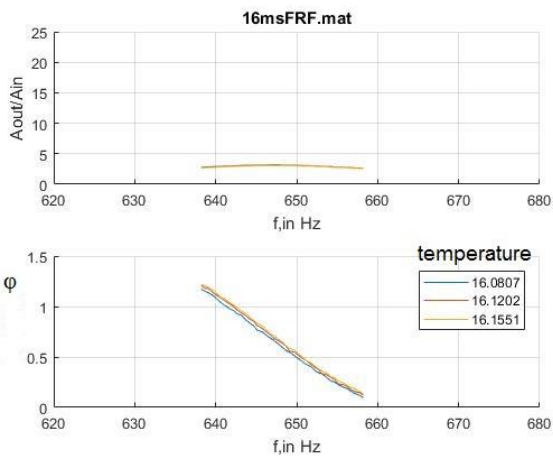
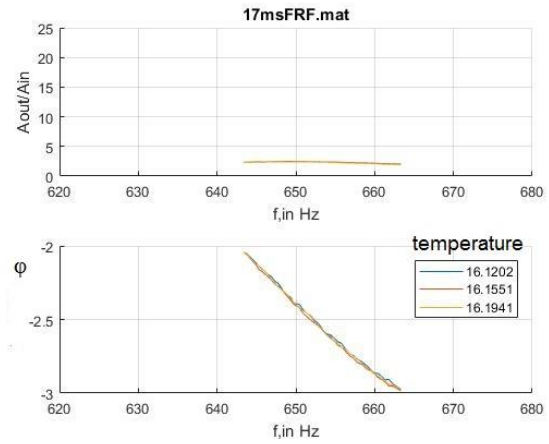
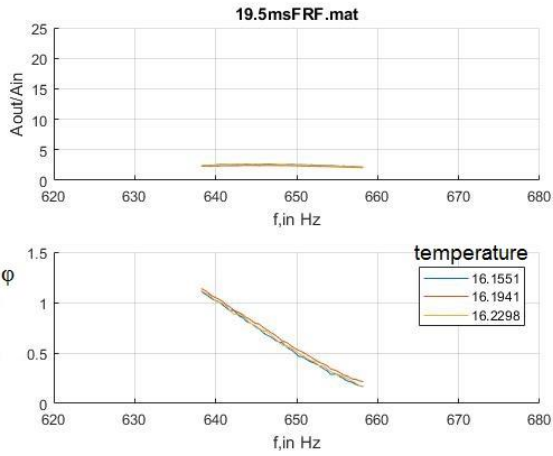
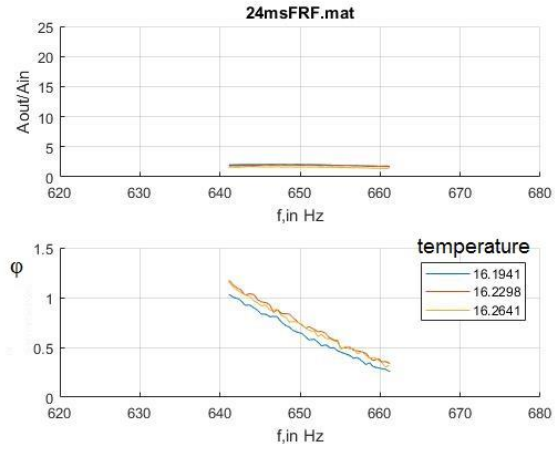
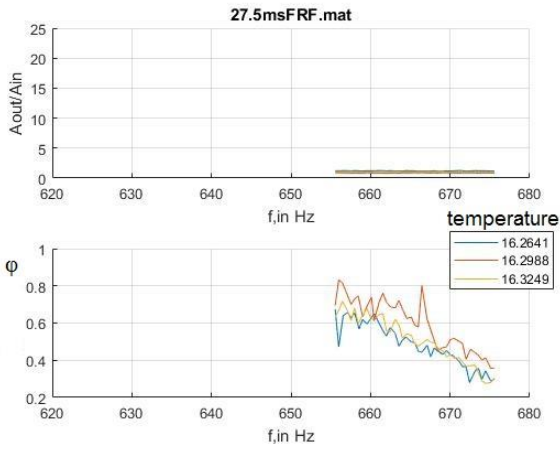
1. 3 repetitions

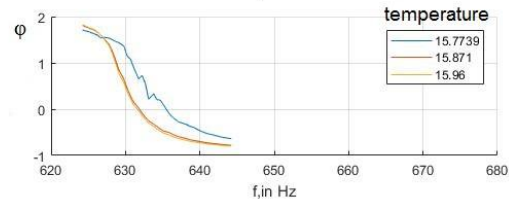
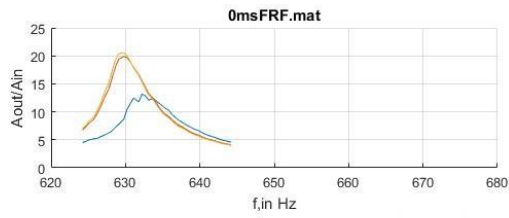
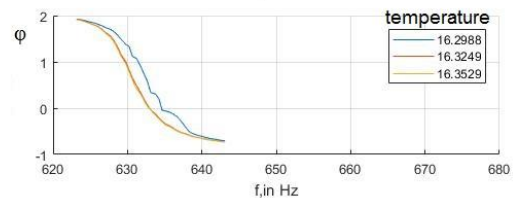
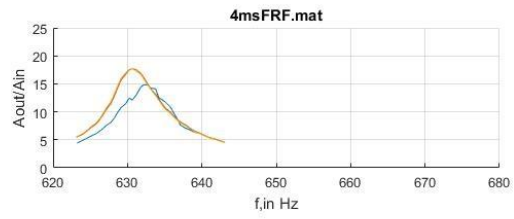
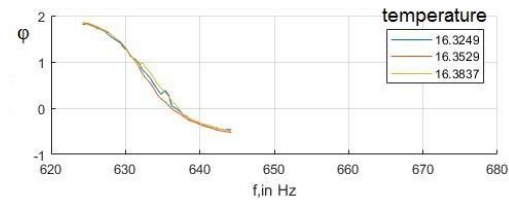
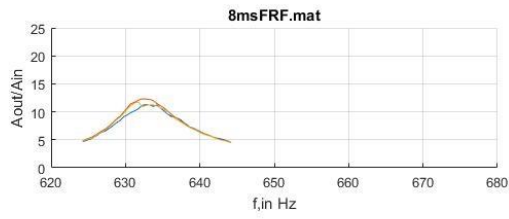
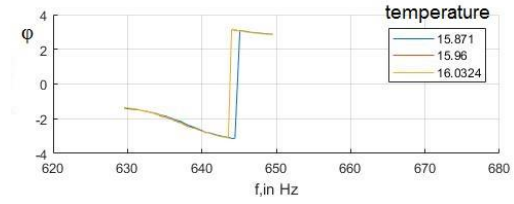
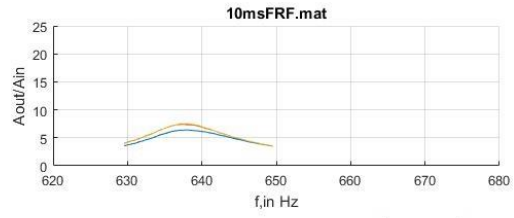
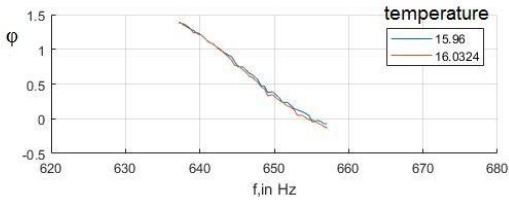
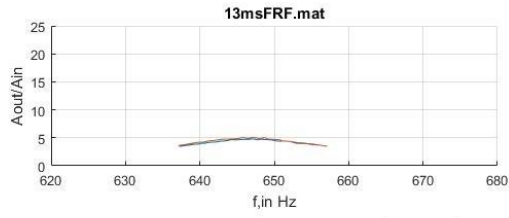
a) F_{LDV}





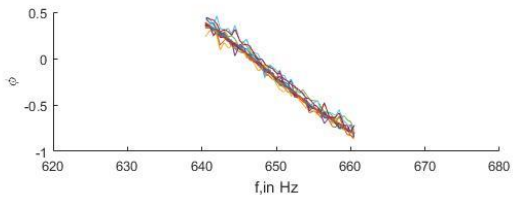
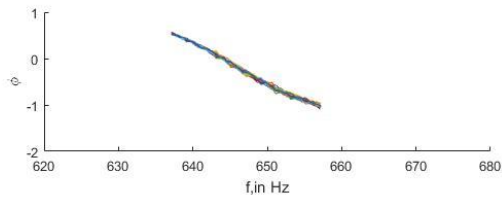
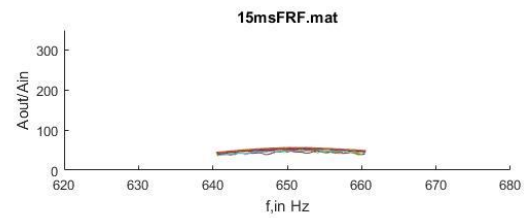
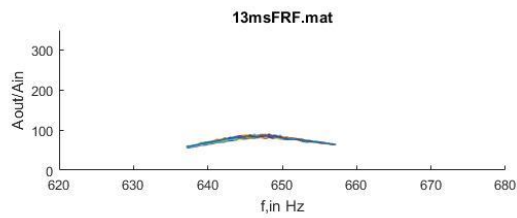
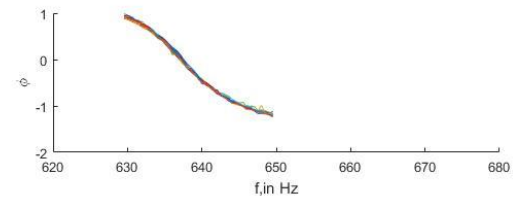
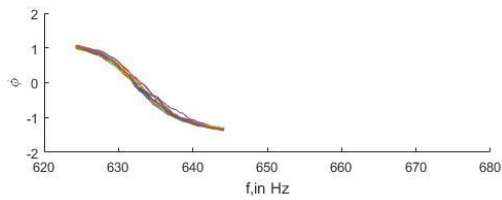
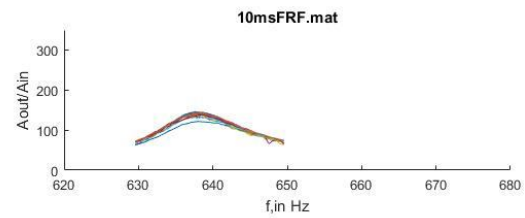
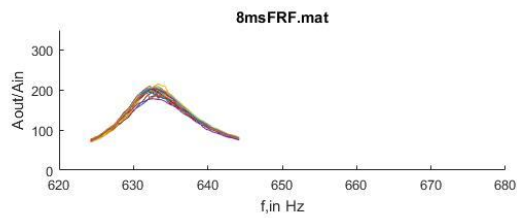
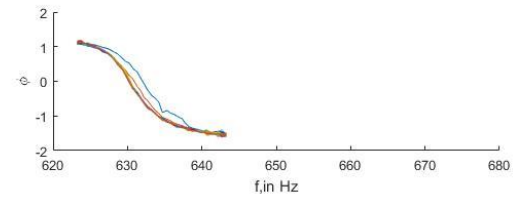
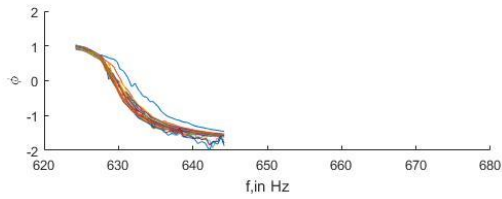
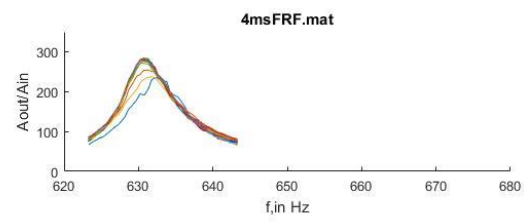
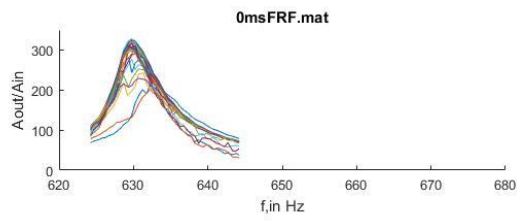
b) *F*_STRAIN

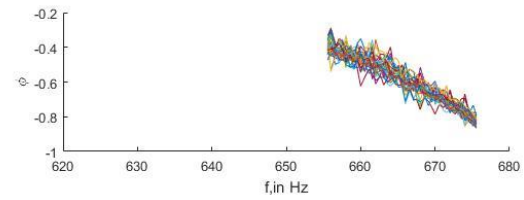
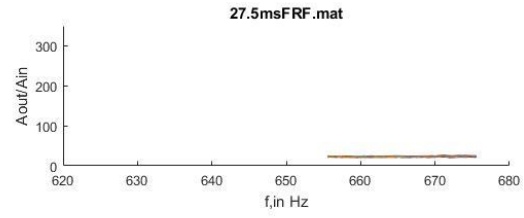
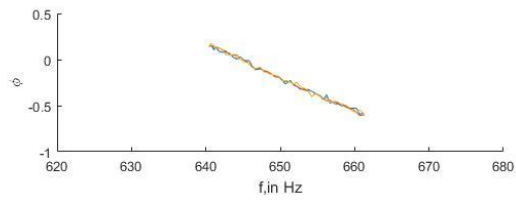
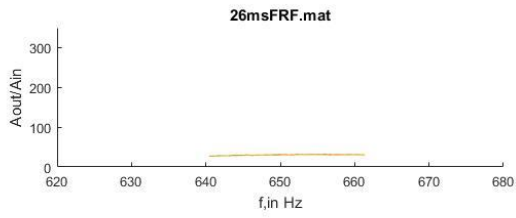
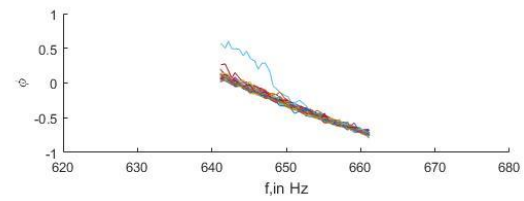
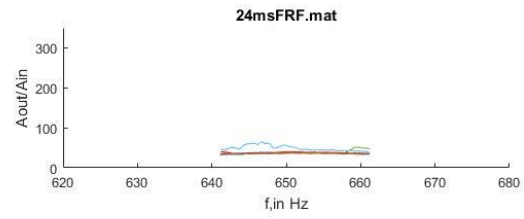
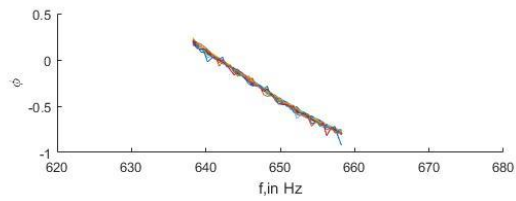
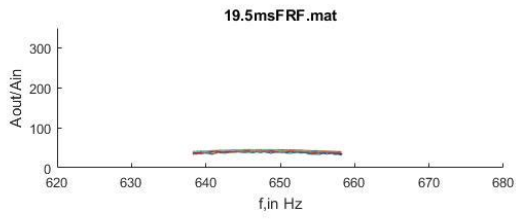
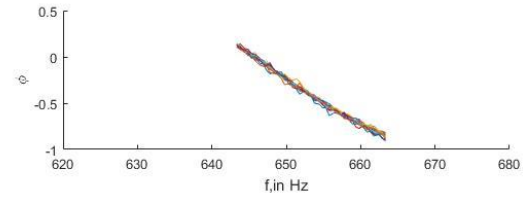
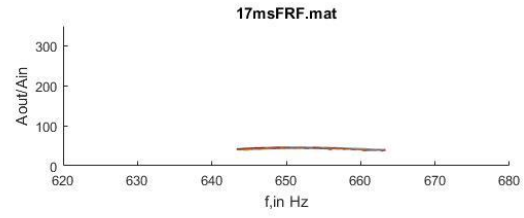
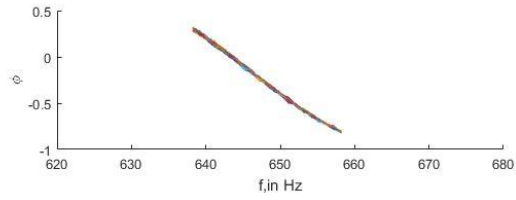
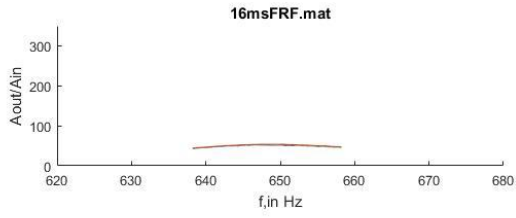




2. For all repetitions

a) F_{LDV}





b) *F*_STRAIN

